

Serveur Académique Lausannois SERVAL serval.unil.ch

Author Manuscript

Faculty of Biology and Medicine Publication

This paper has been peer-reviewed but does not include the final publisher proof-corrections or journal pagination.

Published in final edited form as:

Title: Predictive Patterns of Glutamine Synthetase Immunohistochemical Staining in CTNNB1-mutated Hepatocellular Adenomas.

Authors: Sempoux C, Gouw ASH, Dunet V, Paradis V, Balabaud C, Bioulac-Sage P

Journal: The American journal of surgical pathology

Year: 2021 Feb 8

DOI: 10.1097/PAS.0000000000001675

In the absence of a copyright statement, users should assume that standard copyright protection applies, unless the article contains an explicit statement to the contrary. In case of doubt, contact the journal publisher to verify the copyright status of an article.

American Journal of Surgical Pathology
PREDICTIVE PATTERNS OF GLUTAMINE SYNTHETASE
IMMUNOHISTOCHEMICAL STAINING IN CTNNB1 MUTATED HEPATOCELLULAR
ADENOMAS
 --Manuscript Draft--

Manuscript Number:	AJSP-D-20-00706R2
Full Title:	PREDICTIVE PATTERNS OF GLUTAMINE SYNTHETASE IMMUNOHISTOCHEMICAL STAINING IN CTNNB1 MUTATED HEPATOCELLULAR ADENOMAS
Article Type:	Original Article
Keywords:	Hepatocellular adenoma Beta-catenin activated hepatocellular adenoma Beta-catenin activated Inflammatory hepatocellular adenoma Inflammatory hepatocellular adenoma Glutamine synthetase CD34 Immunohistochemistry Molecular analysis
Corresponding Author:	Christine Sempoux, MD PhD Centre Hospitalier Universitaire Vaudois Lausanne, SWITZERLAND
Corresponding Author Secondary Information:	
Corresponding Author's Institution:	Centre Hospitalier Universitaire Vaudois
Corresponding Author's Secondary Institution:	
First Author:	Christine Sempoux, MD PhD
First Author Secondary Information:	
Order of Authors:	Christine Sempoux, MD PhD Annette S.H. Gouw, MD PhD Vincent Dunet, MD Valérie Paradis, MD PhD Charles Balabaud, MD Paulette Bioulac-Sage, MD
Order of Authors Secondary Information:	
Abstract:	Some hepatocellular adenoma (HCA) subtypes are characterized by different CTNNB1 mutations, leading to different beta-catenin activation levels, hence variable immunostaining patterns of glutamine synthetase (GS) expression, and different risk of malignant transformation. In a retrospective multicentric study of 63 resected inflammatory (n=33) and non-inflammatory (n=30) molecularly confirmed CTNNB1-mutated b-(I)HCA, we investigated the predictive potential of 3 known GS patterns as markers for the CTNNB1 exons 3, 7/8 mutations. Pattern 1 (diffuse homogenous) allowed recognition of 17/21 exon 3 non-S45 mutated b-(I)HCA. Pattern 2 (diffuse heterogeneous) identified all b-(I)HCA harboring exon 3 S45 mutation (20/20). Pattern 3 (focal patchy) distinguished 12/22 b-(I)HCA with exon 7/8 mutations. In exons 3 S45 and 7/8 mutations, both b-HCA and b-IHCA showed a GS+/CD34- rim with diffuse CD34 positivity in the center of the lesion. Inter-observer reproducibility was excellent for exon 3 mutations. Comparative analysis of GS patterns with molecular data showed 83 and 80% sensitivity (b-HCA/b-IHCA) and 100% specificity for exon 3 non-S45. For exon 3 S45, sensitivity was 100% for b-(I)HCA, and specificity 93% and 92% (b-HCA/b-IHCA). For exon 7/8, sensitivity was

55% for both subtypes and specificity 100% and 96% (b-HCA/b-IHCA). Preliminary data from 16 preoperative needle biopsies from the same patients suggest that this panel may also be applicable to small samples.

In surgically resected HCA, two distinct GS patterns can reliably predict CTNNB1 exon 3 mutations, which are relevant due to the higher risk for malignant transformation. The third pattern, although specific, was less sensitive for identification of exon 7/8 mutation, but the GS+/CD34- rim is a valuable aid to indicate either an exon 3 S45 or exon 7/8 mutation.

**PREDICTIVE PATTERNS OF GLUTAMINE SYNTHETASE IMMUNOHISTOCHEMICAL
STAINING IN *CTNNB1* MUTATED HEPATOCELLULAR ADENOMAS**

Christine Sempoux MD, PhD^{1*}, Annette S.H. Gouw MD, PhD^{2*}, Vincent Dunet MD³,
Valérie Paradis MD, PhD⁴, Charles Balabaud⁵ MD, Paulette Bioulac-Sage⁵ MD

1. Service of Clinical Pathology, Institute of Pathology, Lausanne University Hospital and University of Lausanne, Rue du Bugnon 25, 1011, Lausanne, Switzerland. orcid.org/0000-0003-1375-3979
2. Department of Pathology and Medical Biology, University Medical Center Groningen, HPC EA10, PO Box 30.001, 9700 RB, Groningen, the Netherlands. orcid.org/0000-0002-8710-3445
3. Department of Diagnostic and Interventional Radiology, Lausanne University Hospital and University of Lausanne, Lausanne, Switzerland orcid.org/0000-0002-9897-4561
4. Department of Pathology, Beaujon Hospital, 100 Boulevard General Leclerc Clichy, France orcid.org/0000-0003-3142-3762
5. Université of Bordeaux, INSERM, BaRITOn, U1053, F-33000 Bordeaux, France. P Bioulac-Sage orcid.org/0000-0001-5952-0623 C Balabaud orcid.org/0000-0003-0081-8112

* These two authors contributed equally to this work

Corresponding author

Prof. Christine Sempoux,
Service of Clinical Pathology, Institute of Pathology,

1
2
3
4
5
6
7
8
9
10
11
12
13
14
15
16
17
18
19
20
21
22
23
24
25
26
27
28
29
30
31
32
33
34
35
36
37
38
39
40
41
42
43
44
45
46
47
48
49
50
51
52
53
54
55
56
57
58
59
60
61
62
63
64
65

Lausanne University Hospital,

Rue du Bugnon 25, 1011, Lausanne, Switzerland.

Tel/Fax: +41 (0)21 314 71 11 / +41 (0)21 314 71 15.

E-mail: christine.sempoux@chuv.ch.

Conflict of interest

Authors report nothing to disclose

Abstract

1
2 Some hepatocellular adenoma (HCA) subtypes are characterized by different
3
4 *CTNNB1* mutations, leading to different beta-catenin activation levels, hence variable
5
6 immunostaining patterns of glutamine synthetase (GS) expression, and different risk
7
8 of malignant transformation. In a retrospective multicentric study of 63 resected
9
10 inflammatory (n=33) and non-inflammatory (n=30) molecularly confirmed *CTNNB1*-
11
12 mutated b-(I)HCA, we investigated the predictive potential of 3 known GS patterns as
13
14 markers for the *CTNNB1* exons 3, 7/8 mutations.
15
16

17
18
19 Pattern 1 (diffuse homogenous) allowed recognition of 17/21 exon 3 non-S45 mutated
20
21 b-(I)HCA. Pattern 2 (diffuse heterogeneous) identified all b-(I)HCA harboring exon 3
22
23 S45 mutation (20/20). Pattern 3 (focal patchy) distinguished 12/22 b-(I)HCA with exon
24
25 7/8 mutations. In exons 3 S45 and 7/8 mutations, both b-HCA and b-IHCA showed a
26
27 GS+/CD34- rim with diffuse CD34 positivity in the center of the lesion. Inter-observer
28
29 reproducibility was excellent for exon 3 mutations. Comparative analysis of GS
30
31 patterns with molecular data showed 83 and 80% sensitivity (b-HCA/b-IHCA) and
32
33 100% specificity for exon 3 non-S45. For exon 3 S45, sensitivity was 100% for b-
34
35 (I)HCA, and specificity 93% and 92% (b-HCA/b-IHCA). For exon 7/8, sensitivity was
36
37 55% for both subtypes and specificity 100% and 96% (b-HCA/b-IHCA). Preliminary
38
39 data from 16 preoperative needle biopsies from the same patients suggest that this
40
41 panel may also be applicable to small samples.
42
43
44
45
46
47

48
49 In surgically resected HCA, two distinct GS patterns can reliably predict *CTNNB1* exon
50
51 3 mutations, which are relevant due to the higher risk for malignant transformation. The
52
53 third pattern, although specific, was less sensitive for identification of exon 7/8
54
55 mutation, but the GS+/CD34- rim is a valuable aid to indicate either an exon 3 S45 or
56
57 exon 7/8 mutation.
58
59
60
61
62
63
64
65

Introduction

Hepatocellular adenomas (HCA) are rare, benign hepatocellular neoplastic lesions, predominantly occurring in female patients in their reproductive age, usually after prolonged use of oral contraception.¹ The two major complications of HCA are hemorrhage and malignant transformation, developing in 15-25%^{2,3} and 5-8%^{2, 4-7} of the cases, respectively. HCAs are molecularly categorized in different genotypes and the subsequent altered expression of several proteins in the tumor provides the possibility to recognize the HCA subtypes using immunohistochemical (IHC) analyses.⁷ Malignant transformation of HCA in hepatocellular carcinoma (HCC) is more frequent in males² and in some clinical contexts such as vascular liver diseases⁸, androgen consumption⁹ or metabolic disorders.¹⁰ It also depends on mutations in the *CTNNB1* gene.¹¹

There are different types of *CTNNB1* mutations in HCA, leading to variable levels of beta-catenin activation, hence to different levels of increased risk of malignant transformation.¹ Mutations in exon 3 of the *CTNNB1* gene, leading to a strong activation of the Wnt/b-catenin pathway, are associated with a high risk for development of HCC whereas mutations in exons 7 and 8 display low risk of malignant transformation.² Both the recognition of a *CTNNB1* mutation in HCA and correct identification of the type of mutation are relevant for clinical management, since imaging is as yet unable to recognize such subtypes. Molecular analysis of tumor tissue samples both on frozen⁴ and on formalin-fixed paraffin-embedded (FFPE) materials^{12,13} is not as widely available in routine practice as immunohistochemistry,

1 and if the technique is available, the molecular analysis does not always include
2 *CTNNB1* exons 7 and 8 mutations.
3

4 Nuclear beta-catenin expression, the IHC hallmark of exon 3 *CTNNB1* mutation, is
5 regarded as an inadequate marker for beta-catenin activation due to its low sensitivity,
6
7 in contrast with the recognized suitability of glutamine synthetase (GS), a target protein
8
9 of the *CTNNB1* gene, as a surrogate IHC marker for b-catenin mutation.^{7,14} Several
10
11 studies have documented patterns of GS IHC expression that seem to distinguish the
12
13 different *CTNNB1* mutations.^{11,15-16} However, the lack of consensus on the terminology
14
15 of the different GS staining patterns and on the criteria for their application and
16
17 interpretation impedes a standardized and common application of GS as a predictive
18
19 marker for *CTNNB1* mutations in HCA.¹⁷⁻¹⁸ In addition, it is still unclear whether the GS
20
21 immunostaining pattern is similar in beta-catenin mutated HCA (b-HCA) and beta-
22
23 catenin mutated inflammatory HCA (b-IHCA) when harboring the same type of
24
25 *CTNNB1* mutation.
26
27
28
29
30
31
32
33

34 The current study was undertaken to address these issues, by evaluation of specific
35
36 patterns of GS IHC expression associated with exons 3, 7 and 8 *CTNNB1* mutations
37
38 in b-HCA and b-IHCA. We studied the predictive value of GS immunostaining as the
39
40 marker of *CTNNB1* mutations and established its potentials and limitations for routine
41
42 practice. In addition, we assessed the additional and complementary role for CD34,
43
44 which had only been described in a few case reports and reviews.^{15, 19-20} In particular,
45
46 we evaluated the role of a GS positive CD34 negative rim at the periphery of the tumor,
47
48 previously observed in HCA with exon 3 S45 and exons 7/8 mutations.²¹ Only b-HCA
49
50 and b-IHCA subtypes were included because the incidence and consequences of
51
52 *CTNNB1* mutations in these two subgroups of HCA are well established, which is not
53
54 the case in the other subtypes. Although it has been shown that HNF1 α -inactivated
55
56
57
58
59
60
61
62
63
64
65

1 HCA (H-HCA) ²² or sonic-hedgehog HCA (shHCA) ²³ can undergo malignant
2 transformation, there is so far no identified role for *CTNNB1* in these subtypes, hence
3
4 the interpretation of GS staining in that context should be made with caution. We
5
6 included inflammatory HCA (IHCA) as controls, for comparison with b-IHCA. In this
7
8 study, we follow the concept, which we regard as mandatory for routine practice, that
9
10 the diagnosis and subtyping of HCA should be performed using conventional
11
12 hematoxylin and eosin (H&E) staining and ancillary immunohistology ⁷ before
13
14 proceeding to the interpretation of GS expression.
15
16
17
18

19 **Materials and Methods**

20
21 This is a retrospective multicentric study of 111 surgically resected b-HCA, b-IHCA and
22
23 IHCA, collected from 4 departments of Pathology: CHU Bordeaux (Bordeaux, France,
24
25 76 cases), University Medical Center Groningen (Groningen, the Netherlands, 8
26
27 cases), Beaujon Hospital (Paris, France, 5 cases), and Lausanne University Hospital
28
29 (Lausanne, Switzerland, 4 cases). In all centers, patients had been informed and/or
30
31 given their consent for using their anonymized data for scientific purposes.
32
33
34
35

36 Inclusion was based on the availability of the following elements. It was mandatory to
37
38 have the molecular data of *CTNNB1* mutations of exons 3, 7 and 8 as the gold
39
40 standard, performed on frozen or FFPE tissues. Mutations in exon 3 were differentiated
41
42 in mutations at the hot spot S45 on one side, and other mutations or deletion referred
43
44 as “exon 3 non-S45” on the other side. Exons 7 and 8 mutations were pooled in the
45
46 same group. IHC of C-reactive protein and/or serum amyloid A (CRP/SAA) was
47
48 available in all cases to recognize the IHCA and b-IHCA. GS and CD34 IHC were
49
50 evaluated on samples containing the interface between lesional and non-lesional liver
51
52 tissue. HCA with extensive hemorrhage or necrosis were excluded, except if there was
53
54 an area of enough viable tissue. In case of an existing associated HCC, only the HCA
55
56
57
58
59
60
61
62
63
64
65

1 part was studied. The IHC techniques and applied antibodies have been described
2 previously¹⁴ and are fully comparable in the 4 participating centers.
3

4 The observers assessed all cases individually and blinded to the clinical and mutational
5 data. The individual microscopic analysis was preceded by a short introduction
6 organized as a jointly histological session at the multi-head microscope using 10 of the
7 93 cases to reach an agreement regarding the different patterns of GS staining,
8 derived from the work of Rebouissou *et al.*¹¹, and depicted in Figure 1.
9

10
11
12
13
14
15
16 **Pattern 1**, the ***diffuse homogeneous GS pattern*** corresponds to a diffuse, moderate
17 to strong, GS expression in all lesional hepatocytes, often associated with the
18 presence of various number of beta-catenin positive nuclei and an increased but non-
19 diffuse CD34 staining of the sinusoids. Molecularly, this pattern had been associated
20 with either large deletions or mutations in exon 3 (outside the hotspot S45) of *CTNNB1*
21 gene, corresponding mainly to T41 or D-32-S37 mutations.¹¹
22
23
24
25
26
27
28
29
30

31 **Pattern 2**, the ***diffuse heterogeneous GS pattern***, shows GS expression of variable
32 intensity in a majority of individual hepatocytes distributed diffusely in the entire lesion,
33 giving a “starry sky” impression, at lower power.⁷ In addition, a strong GS positive but
34 CD34 negative rim is seen at the border of the HCA, with a contrasting diffuse positive
35 CD34 expression in the center of the lesion. None or just a few beta-catenin positive
36 nuclei were found. This second type of IHC pattern had been associated with *CTNNB1*
37 exon 3 S45 mutation.¹¹
38
39
40
41
42
43
44
45
46
47

48 **Pattern 3**, the ***focal patchy GS pattern***, is characterized by a faint GS staining in few
49 hepatocytes irregularly scattered within the HCA, often associated with a variable
50 number of GS positive patches of predominantly perivenular hepatocytes. This pattern
51 is again associated with a GS positive-CD34 negative rim at the border between the
52 HCA and the normal liver, and with the same contrasting feature of diffuse CD34
53
54
55
56
57
58
59
60
61
62
63
64
65

positivity in the center. Nuclear beta-catenin positivity was absent. This pattern had been associated with exon 7 or 8 *CTNNB1* K335 or N387 point mutations.¹¹

Absence of *CTNNB1* mutations is associated with absence of GS expression, except around some veins or occasional patches within the HCA or at its periphery, with absence of a well-defined GS rim. CD34 expression is unremarkable.

The algorithm describing the different staining patterns corresponding to the *CTNNB1* mutations presented in Figure 2 summarizes the scoring workflow used for this study. For each case, the evaluation started by subtyping the HCA into IHCA or non-IHCA, according to the CRP/SAA immunostaining followed by the evaluation of GS, beta-catenin and CD34 immunostainings. After individual evaluations of all cases, discordant results were discussed at the multi-head microscope to reach a final consensus, still blinded to the molecular results to assess the inter-observer reproducibility. Hereafter, the conclusions were reconciled with the molecular data to define the sensitivity and the specificity of the 3 GS IHC patterns of staining.

Statistical analysis

All statistics were performed using the Stata 13.1 software (StataCorp, College Station, Texas, USA). Continuous variables are displayed as mean \pm standard deviation (SD) and categorical variables as number or percentage. Inter-observer reproducibility between the readers was tested for the seven subtypes defined by molecular analysis. To this purpose, we used the unweighted Gwet's AC1 coefficient corrected for chance agreement in order to overcome the two paradoxes of the Cohen's kappa (i.e. (1) low kappa despite high agreement under highly symmetrically imbalanced marginals and (2) higher kappa values for asymmetrical imbalanced marginal distributions.²⁴⁻²⁵ We used a modified Landis and Koch scale to characterize the value of the Gwet's AC1 coefficient, as follows: poor when Gwet's AC1 was <0.00 , slight between 0.00 and

0.20, fair between 0.21 and 0.40, moderate between 0.41 and 0.60, good between 0.61 and 0.80 and excellent above 0.81. Finally, the diagnostic performance of consensus was evaluated by calculating sensitivity, specificity, positive and negative predictive values, and area under the curve (AUC) with respective 95% confidence interval (95%CI) for each subtype considering molecular analysis as the gold standard. P-value<0.05 was considered statistically significant.

Results

Ninety-three HCA samples from 87 patients (11 men, age range: 14-59 years, median 35 years; 76 women, age range: 19-66 years, median 33 years) fitted the inclusion criteria (Table 1). One woman had 3 HCAs and four women had 2 HCAs included in the series. Sixty-three samples were inflammatory HCA (33 b-IHCA and a control group of 30 IHCA) and 30 were b-HCA. Based on the molecular data, 15/33 b-IHCA samples had *CTNNB1* exon 3 non-S45 mutation, 7 samples had exon 3 S45 mutation and 11 samples had exon 7 or 8 mutations. Of the 30 b-HCA samples, 6 had exon 3 non-S45 mutation, 13 had exon 3 S45 mutation and 11 samples had exon 7 or 8 mutation (Table 1). Four cases were associated with an existing HCC (2 b-HCA exon 3 non-S45, 1 b-HCA exon 3 S45 and 1 b-IHCA exon 3 non-S45). In 3 of these 4 cases and in 6 additional cases (2 b-HCA exon 3 non-S45, 1 b-HCA exon 3 S45, 2 b-IHCA exon 3 non-S45 and 1 b-IHCA exon 3 S45), the HCAs showed some focal cytoarchitectural atypia yet insufficient to reach the diagnosis of HCC. None had *TERT* promoter mutation.

Pattern 1: Diffuse homogeneous GS pattern (Figure 3).

This pattern allowed recognition of 5/6 b-HCA and 12/15 b-IHCA with *CTNNB1* exon 3 non-S45 mutation with an excellent inter-observer reproducibility (AC1 values of 0.87 [95%CI: 0.48-1.0] for b-HCA and 0.90 [95%CI: 0.74-1.0] for b-IHCA). There was an

1
2
3
4
5
6
7
8
9
10
11
12
13
14
15
16
17
18
19
20
21
22
23
24
25
26
27
28
29
30
31
32
33
34
35
36
37
38
39
40
41
42
43
44
45
46
47
48
49
50
51
52
53
54
55
56
57
58
59
60
61
62
63
64
65

excellent sensitivity of 83% (95%CI: 36-99%) for b-HCA and 80% (95%CI: 52-96%) for b-IHCA whilst the specificity rate was 100% (95%CI: 95-100%) for both types. The GS staining intensity was strong (Fig 3A). CD34 staining was increased but never diffuse (Fig 3B). Scattered beta-catenin positive nuclei were found but were not applied as key decision-making feature. In this group there were no differences in the GS and CD34 patterns between b-HCA and b-IHCA. In the group of 21 HCA harboring an underlying *CTNNB1* exon 3 non-S45 mutation, 1 b-HCA case and 3 b-IHCA cases were wrongly interpreted as having an exon 3 S45 mutation because of some heterogeneity in the intensity of the GS staining at lower power.

Pattern 2: Diffuse heterogeneous GS pattern (Figure 4).

This GS pattern, associated with diffuse CD34 staining in the center of the lesion, and a strong GS positive-CD34 negative rim at the lesional border area, allowed a perfect recognition of the 13/13 b-HCA and 7/7 b-IHCA cases with *CTNNB1* exon 3 S45 mutation (Fig. 4A, 4B, 4C). Inter-observer reproducibility was excellent (AC1 values of 0.96 [95%CI: 0.87-1.0] for b-HCA and 0.89 [95%CI: 0.58-1.0] for b-IHCA). This pattern and the rim proved to be highly sensitive (100% [95%CI: 59-100%] for both types of HCA). A 93% (95%CI: 84-97%) specificity rate was reached for b-HCA and 92% (95%CI: 84-97%) for b-IHCA. Intensity of the GS staining within the HCA was variable (Fig 4D, 4E, 4F) which did not impede the recognition of the pattern. In b-IHCA, the rim was sometimes less well-defined, and CD34 in the center was not always as diffuse as in b-HCA. The excellent sensitivity reflects that all cases containing exon 3 S45 mutation were correctly detected. The slightly less specificity results from wrongly diagnosed cases: 1 b-HCA and 3 b-IHCA exon 3 non-S45 (described in the previous paragraph), 5 b-HCA and 3 b-IHCA exon 7/8, and 1 IHCA (see below).

Pattern 3: Focal patchy GS pattern (Figure 5).

1 This pattern, accompanied by a GS positive-CD34 negative rim and a diffuse CD34
2 expression in the center, identified 6/11 b-HCA and 6/11 b-IHCA with *CTNNB1* exon
3 7/8 mutations (Fig. 5A, 5B, 5C, 5D). A moderate inter-observer reproducibility was
4 reached for b-HCA (AC1= 0.46, 95%CI: -0.03-0.96) whereas it was good for b-IHCA
5 (AC1=0.67, 95%CI: 0.35-0.98). The sensitivity of the criteria for the identification of b-
6 HCA exon 7/8 was 55% (95%CI: 23-83%) with a 100% (95%CI: 96-100%) specificity.
7 For b-IHCA, the sensitivity was also 55% (95%CI: 23-83%) with a 96% (95%CI: 90-
8 99%) specificity. In contrast with b-HCA, b-IHCA with exon 7/8 mutation often showed
9 a less well-defined rim, and larger perivascular GS positive areas in the tumoral center.
10 Five b-HCA and 3 b-IHCA were wrongly considered as having exon 3 S45 mutations
11 (see previous paragraph), and 2 b-IHCA were considered as IHCA. In addition, 3 IHCA
12 were wrongly interpreted as b-IHCA exon 7/8 mutation (see below).
13
14
15
16
17
18
19
20
21
22
23
24
25
26
27
28

29 One additional observation made in case of *CTNNB1* exon 3 S45 and exon 7/8
30 mutations, in b-HCA more often than in b-IHCA, was the presence of a focal increase
31 in large irregular vessels in the CD34 positive area, usually not far from the rim.
32
33
34
35

36 **IHCA without *CTNNB1* mutation (Figure 6)**

37 All but 4 of 30 IHCA cases were correctly interpreted as devoid of *CTNNB1* mutation.
38 GS expression was negative in most cases, with mainly some perivascular expression
39 in comparable extents as in the non-lesional counterpart, or slightly increased, at the
40 periphery of the tumor (Fig. 6A) but without a well-defined GS positive-CD34 negative
41 rim. The CD34 expression was patchy and unremarkable (Fig. 6B). Application of
42 these “negative” criteria resulted in a good inter-observer reproducibility (AC1= 0.74,
43 95%CI: 0.61-0.88). The sensitivity and specificity of consensus were 87% (95%CI: 69-
44 96%) and 97% (95%CI: 89-100%) respectively. As mentioned earlier, 3 cases were
45 wrongly interpreted as having exon7/8 mutation and 1 case as exon 3 S45. However,
46
47
48
49
50
51
52
53
54
55
56
57
58
59
60
61
62
63
64
65

1 at reassessment, no fully developed GS positive-CD34 negative rim was present which
2 should have signaled the lack of *CTNNB1* mutation.
3

4 When only the total group of inflammatory HCA (IHCA and b-IHCA, n=63) is
5 considered, the specificity and the sensitivity to predict the presence of a *CTNNB1*
6 mutation was excellent, 87% (95%CI: 69-96%) and 94% (95%CI: 80-99%)
7 respectively.
8
9

10 In the assessment of the individual evaluations of the observers, concordance was
11 present for 66 HCAs (71%), and differences were found in 27 lesions. In 14/27, only
12 one observer was divergent, and, at joint reassessment, consensus was reached,
13 leading to a total agreement for 80/93 cases (86%). In 9 of these 80 cases (11%), there
14 was a mismatch with the molecular data. In the 13/93 cases with complete divergent
15 evaluations, the consensus that was reached did not match with the molecular analysis
16 in 9/13 (69%) cases (Table 1). Table 2 summarizes the statistical results.
17
18
19
20
21
22
23
24
25
26
27
28
29
30

31 **Discussion**

32 In this multicenter study of the GS IHC patterns as a predictive marker for *CTNNB1*
33 exons 3 and 7/8 mutations in 33 b-IHCA and 30 b-HCA with established *CTNNB1*
34 molecular data, we reached excellent levels of inter-observer reproducibility and high
35 sensitivity and specificity degrees for the mutations of exon 3 non-S45 and exon 3 S45
36 variants. However, GS IHC alone is not reliable enough to recognize b-(I)HCA with
37 mutation in exon 7/8. This is compensated by our confirmation of the specific feature
38 of the GS positive-CD34 negative rim in exon 7/8 and exon 3 S45 mutated b-(I)HCA
39 which is a valuable aid to recognize that an HCA has an underlying *CTNNB1* mutation.
40
41
42
43
44
45
46
47
48
49
50
51

52 **Pattern 1, the diffuse homogenous GS pattern** is specifically associated with exon
53 3 non-S45 mutation and is recognizable and reproducible in both b-HCA and b-IHCA.
54
55
56
57
58
59
60
61
62
63
64
65

1
2
3
4
5
6
7
8
9
10
11
12
13
14
15
16
17
18
19
20
21
22
23
24
25
26
27
28
29
30
31
32
33
34
35
36
37
38
39
40
41
42
43
44
45
46
47
48
49
50
51
52
53
54
55
56
57
58
59
60
61
62
63
64
65

Using this pattern an exon 3 non-S45 mutation should not be missed because of the high risk of malignant transformation of this category.

Four cases with exon 3 non-S45 mutations were misdiagnosed as exon 3 S45, but retrospectively, the absence of the GS positive-CD34 negative rim and the patchy CD34 central in the lesions should have prevented the misclassification. The variable intensity, yet still diffuse staining also gave the impression of heterogeneity at lower power. This phenomenon may partly be due to a variant hotspot mutation ¹¹ (e.g. exon 3 P52S, case 38) and may form a pitfall in this category.

Of note, a small number of HCA cases with strongly and diffusely positive GS but without *CTNNB1* mutation analyzed in FFPE samples have been described.^{16,26} This phenomenon can be explained either by known technical issues of the molecular analyses ²⁷, or, it might result from the activation of other pathways. Such cases were not included in this study. Nevertheless, a diffuse and strong GS expression in an HCA (b-HCA or b-IHCA) indicates a strong activation of the beta-catenin pathway. Since the risk of cancer is linked to the level of beta-catenin activation ¹¹, such cases should be carefully followed up.

Pattern 2, the diffuse heterogeneous GS pattern is highly reproducible and reliable to identify *CTNNB1* exon 3 S45 mutations for both b-HCA and b-IHCA. Recognition of this mutational subtype is relevant because of its risk of malignant transformation.^{2,11, 28-29} The reliability in recognizing this diffuse heterogenous pattern (also labelled as “starry sky”) ⁷ whatever the staining intensity (Figure 4D, 4E, 4F), as well as its high sensitivity is demonstrated for the first time in the current study.

An important finding in the current study is the significance of the GS positive-CD34 negative rim that indicates the existence of a *CTNNB1* mutation, either exon 3 S45 or exon 7/8. However, this rim does not distinguish between the 2 types of mutations

1 which can be discriminated by the GS pattern in the central part of the tumor and/or
2 molecular typing. The pathogenetical significance of this rim is not fully understood.
3
4 We hypothesize that it is most probably related to a difference in the vascularization,
5
6 as also underlined by the sharp CD34 staining distinction between the rim and the
7
8 center, indicating differences in sinusoidal capillarization. Interestingly, a strong GS
9
10 positive hyperplastic area has also been described around some hypervascular
11
12 malignant primary or secondary liver tumors.³⁰
13
14
15

16 With regard to **pattern 3, the focal patchy GS pattern**, our results show that the
17
18 identification of exon 7/8 mutation by IHC is of limited reliability. The GS positive-CD34
19
20 negative rim will indicate an underlying *CTNNB1* mutation (Figure 5A-5D) although
21
22 confirmation of an exon 7/8 mutation will require molecular typing in 50% of the cases.
23
24 Establishing exon 7/8 mutation is relevant as the potential for malignant transformation
25
26 is indeed low but not negligible, as shown in a recent case report.³¹ This particular case
27
28 also had *TERT* promoter mutation indicating an additional genetic event contributing
29
30 to malignant transformation.
31
32
33
34
35

36 The criteria that we have applied in the current study are only applicable in a strict
37
38 systematic analysis starting by the recognition of the lesion as an HCA and not an HCC
39
40 because other criteria should be applied for the latter.³² Since the significance of GS
41
42 expression in the other subtypes of HCA, i.e. H-HCA and shHCA is still unknown, the
43
44 second step is to subtype the HCA and it is only after this second step that it is possible
45
46 to proceed with the interpretation of the GS staining together with CD34, as proposed
47
48 in our algorithm (Figure 2). Taken together, our results showed that the criteria are
49
50 applicable to effectively recognize the 2 subtypes of exon 3 mutation in b-(I)HCA which
51
52 represent the group with the highest risk of malignant transformation. Of equal clinical
53
54 importance is our finding that GS staining is also a suitable method to identify the
55
56
57
58
59
60
61
62
63
64
65

1 absence of *CTNNB1* mutations in IHCA. Molecular biology remains mandatory in HCA
2 cases showing inconclusive immunohistology.
3

4 The strength of our study is that it is strictly based on molecular data. However, there
5 are several limitations. First, we analyzed surgical specimens only, to guarantee the
6 availability of the marginal area between lesional and non-lesional liver. This necessary
7 first step approach means that the applicability of the criteria on biopsy specimens
8 remains to be established. After completion of the study, we assessed the 16 available
9 pre-resection biopsies (3IHCA, 13 b-(l)HCA) of the current cohort. Our preliminary data
10 in this very limited number of biopsies show that the patterns we described can indeed
11 be discerned in biopsies, especially in the IHCA and exon 3 mutated cases; but, as in
12 the resection specimens, recognition of the exon 7/8 mutated cases was incomplete
13 (data not shown). However, these data are too limited and are also subject to recall
14 bias, to allow application on biopsies at this stage. Such an application will need a
15 prospective and specific biopsy study, with a different larger cohort that should also
16 include focal nodular hyperplasia (FNH) and HCA without *CTNNB1* mutations. With
17 regard to FNH, we can already anticipate on the difficult differential diagnosis on a
18 needle biopsy between the GS rim of *CTNNB1* exon 3 S45 and exon 7/8 mutated HCA
19 and the GS map-like pattern of FNH. A second limitation is that the evaluation of the
20 GS immunostaining patterns was performed by expert liver pathologists with long time
21 experience in HCA analysis and was not compared with the interpretation by general
22 pathologists. However, HCA is a specialized field of medicine, partly due to its rarity,
23 requiring a multidisciplinary approach of specialized teams³³ including dedicated liver
24 pathologists; hence, our study could be considered as representative.
25

26 In conclusion, in an appropriate step-by-step analysis of HCA, recognition of the
27 different GS staining patterns, combined with CD34, is a valuable method to identify
28
29
30
31
32
33
34
35
36
37
38
39
40
41
42
43
44
45
46
47
48
49
50
51
52
53
54
55
56
57
58
59
60
61
62
63
64
65

1 the molecular subgroups of *CTNNB1*-mutated HCA at higher risk of malignant
2 transformation, and represents a useful tool for patient management in routine
3
4 practice. Its application on biopsy samples remains to be validated by a separate study.
5
6

7 **Acknowledgements**

8
9 The authors would like to thank their colleagues who had performed the molecular
10 analyses: Prof. J Zucman-Rossi and Dr. David Cappellen for CHU Bordeaux
11 (Bordeaux, France) and Beaujon Hospital (Paris, France); S. Huitema, Dr. M.C. van
12 den Heuvel (for help in selecting cases) and Prof. A. van den Berg for University
13 Medical Center Groningen (Groningen, the Netherlands), and Dr. B Bisig and Dr .Sc.
14 E Missiaglia for Lausanne University Hospital (Lausanne, Switzerland), as well as Dr.
15
16
17
18
19
20
21
22
23
24 J Calderaro for sharing with the authors his experience in GS interpretation.
25
26
27
28
29
30
31
32
33
34
35
36
37
38
39
40
41
42
43
44
45
46
47
48
49
50
51
52
53
54
55
56
57
58
59
60
61
62
63
64
65

References

- 1
2
3
4
5
6
7
8
9
10
11
12
13
14
15
16
17
18
19
20
21
22
23
24
25
26
27
28
29
30
31
32
33
34
35
36
37
38
39
40
41
42
43
44
45
46
47
48
49
50
51
52
53
54
55
56
57
58
59
60
61
62
63
64
65
1. Nault JC, Bioulac-Sage P, Zucman-Rossi J. Hepatocellular benign tumors-from molecular classification to personalized clinical care. *Gastroenterology*. 2013,144:888-902
2. Nault JC, Couchy G, Balabaud C, et al. Molecular Classification of Hepatocellular Adenoma Associates With Risk Factors, Bleeding, and Malignant Transformation. *Gastroenterology*. 2017,152:880-894
3. van Rosmalen BV, Coelen RJS, Bieze M, et al. Systematic review of transarterial embolization for hepatocellular adenomas. *Br J Surg*. 2017,104:823-835
4. Zucman-Rossi J, Jeannot E, Nhieu JT, et al. Genotype-phenotype correlation in hepatocellular adenoma: new classification and relationship with HCC. *Hepatology*. 2006,43:515-524
5. Stoot JH, Coelen RJ, De Jong MC, et al. Malignant transformation of hepatocellular adenomas into hepatocellular carcinomas: a systematic review including more than 1600 adenoma cases. *HPB (Oxford)*. 2010,12:509-522
6. Farges O, Ferreira N, Dokmak S, et al. Changing trends in malignant transformation of hepatocellular adenoma. *Gut*. 2011,60:85-89
7. Bioulac-Sage P, Kakar S, Nault JC. Hepatocellular adenoma. In: WHO Classification of Tumours. 5thEdition. Digestive System Tumours. Lyon, France: International Agency for Research on Cancer (IARC) Press; 2019:224-228
8. Sempoux C, Paradis V, Komuta M, et al. Hepatocellular nodules expressing markers of hepatocellular adenomas in Budd-Chiari syndrome and other rare hepatic vascular disorders. *J Hepatol*. 2015,63:1173-1180

- 1
2
3
4
5
6
7
8
9
10
11
12
13
14
15
16
17
18
19
20
21
22
23
24
25
26
27
28
29
30
31
32
33
34
35
36
37
38
39
40
41
42
43
44
45
46
47
48
49
50
51
52
53
54
55
56
57
58
59
60
61
62
63
64
65
9. Gupta S, Naini BV, Munoz R, et al. Hepatocellular Neoplasms Arising in Association With Androgen Use. *Am J Surg Pathol.* 2016,40:454-461
10. Jang HJ, Yang HR, Ko JS, et al. Development of Hepatocellular Carcinoma in Patients with Glycogen Storage Disease: a Single Center Retrospective Study. *J Korean Med Sci.* 2020 Jan 6;35 :e5.
11. Rebouissou S, Franconi A, Calderaro J, et al. Genotype-phenotype correlation of *CTNNB1* mutations reveals different b-catenin activity associated with liver tumor progression. *Hepatology.* 2016,64:2047-2061
12. Saldarriaga J, Bisig B, Couchy G, et al. Focal β -catenin mutation identified on formalin-fixed and paraffin-embedded inflammatory hepatocellular adenomas. *Histopathology.* 2017,71:989-993
13. Torbenson M, Lee JH, Choti M, et al. Hepatic adenomas: analysis of sex steroid receptor status and the Wnt signaling pathway. *Mod Pathol.* 2002,15:189-196
14. Bioulac-Sage P, Rebouissou S, Thomas C, et al. Hepatocellular adenoma subtype classification using molecular markers and immunohistochemistry. *Hepatology.* 2007,46:740-748
15. Bioulac-Sage P, Sempoux C, Frulio N, et al. Snapshot summary of diagnosis and management of hepatocellular adenoma subtypes. *Clin Res Hepatol Gastroenterol.* 2019,43:12-19
16. Hale G, Liu X, Hu J, Xu Z, et al. Correlation of exon 3 β -catenin mutations with glutamine synthetase staining patterns in hepatocellular adenoma and hepatocellular carcinoma. *Mod Pathol.* 2016,29:1370-1380
17. Kakar S, Ferrell LD. Glutamine synthetase staining and *CTNNB1* mutation in hepatocellular adenomas. *Hepatology.* 2017,66:2092-2093

- 1
2
3
4
5
6
7
8
9
10
11
12
13
14
15
16
17
18
19
20
21
22
23
24
25
26
27
28
29
30
31
32
33
34
35
36
37
38
39
40
41
42
43
44
45
46
47
48
49
50
51
52
53
54
55
56
57
58
59
60
61
62
63
64
65
18. Rebouissou S, Bioulac-Sage P, Nault JC, et al. Genotype-phenotype correlation of CTNNB1 mutations reveals different b-catenin activity associated with liver tumor progression. *Hepatology*. 2017,66:2093-2094
 19. Bioulac-Sage P, Sempoux C, Balabaud C. Hepatocellular adenoma: Classification, variants and clinical relevance. *Semin Diagn Pathol*. 2017,34:112-125
 20. Cappellen D, Balabaud C, Bioulac-Sage P. A difficult case of β -catenin-mutated hepatocellular adenoma: a lesson for diagnosis. *Histopathology*. 2019,74:355-357
 21. Bioulac-Sage P, Cubel G, Balabaud C, et al. Revisiting the pathology of resected benign hepatocellular nodules using new immunohistochemical markers. *Semin Liver Dis*. 2011,31:91-103
 22. Putra J, Ferrell LD, Gouw ASH, et al. Malignant transformation of liver fatty acid binding protein-deficient hepatocellular adenomas: histopathologic spectrum of a rare phenomenon. *Mod Pathol*. 2020,33:665-675
 23. Sala M, Gonzales D, Leste-Lasserre T, et al. ASS1 Overexpression: A Hallmark of Sonic Hedgehog Hepatocellular Adenomas; Recommendations for Clinical Practice. *Hepatol Commun*. 2020,4:809-824
 24. Wongpakaran N, Wongpakaran T, Wedding D, et al. A comparison of Cohen's Kappa and Gwet's AC1 when calculating inter-rater reliability coefficients: a study conducted with personality disorder samples. *BMC Med Res Methodol*. 2013,13:61
 25. Shankar V, Bangdiwala SI. Observer agreement paradoxes in 2x2 tables: comparison of agreement measures. *BMC Med Res Methodol*. 2014,14:100

- 1
2
3
4
5
6
7
8
9
10
11
12
13
14
15
16
17
18
19
20
21
22
23
24
25
26
27
28
29
30
31
32
33
34
35
36
37
38
39
40
41
42
43
44
45
46
47
48
49
50
51
52
53
54
55
56
57
58
59
60
61
62
63
64
65
26. Longerich T, Endris V, Neumann O, et al. *RSPO2* gene rearrangement: a powerful driver of β -catenin activation in liver tumours. *Gut*. 2019,68:1287-1296
27. Bayard Q, Nault J-C, Zucman-Rossi J. *RSPO2* abnormal transcripts result from read-through in liver tumors with high beta-catenin activation and *CTNNB1* mutations. *Gut*. 2020,69:1152–1153
28. Sempoux C, Bisig B, Couchy G, et al. Malignant transformation of a β -catenin inflammatory adenoma due to an S45 β -catenin-activating mutation present 12 years before. *Hum Pathol*. 2017,62:122-125
29. Vilarinho S, Erson-Omay EZ, Mitchell-Richards K, et al. Exome analysis of the evolutionary path of hepatocellular adenoma-carcinoma transition, vascular invasion and brain dissemination. *J Hepatol*. 2017,67:186-191
30. Arnason T, Fleming KE, Wanless IR. Peritumoral hyperplasia of the liver: a response to portal vein invasion by hypervascular neoplasms. *Histopathology*. 2013,62:458-464
31. Klompenhouwer AJ, Thomeer MGJ, Dinjens WNM, et al. Phenotype or Genotype: Decision-Making Dilemmas in Hepatocellular Adenoma. *Hepatology*. 2019,70:1866-1868
32. Nguyen TB, Roncalli M, Di Tommaso L, et al. Combined use of heat-shock protein 70 and glutamine synthetase is useful in the distinction of typical hepatocellular adenoma from atypical hepatocellular neoplasms and well-differentiated hepatocellular carcinoma. *Mod Pathol*. 2016,29:283-292
33. Blanc JF, Frulio N, Chiche L, et al. Hepatocellular adenoma management: call for shared guidelines and multidisciplinary approach. *Clin Res Hepatol Gastroenterol*. 2015;39:180-187

Legend to figures

Table 1. Cases of the series, grouped by molecular categories.

Table 2. Summary of the statistical results: molecular analysis (gold standard) versus immunohistochemical analysis of the patterns (consensus).

Figure 1. Cartoon representing the different hepatocellular Glutamine Synthetase (GS, brown, left panel) and sinusoidal CD34 (blue, right panel) patterns of staining.

A: Pattern 1: diffuse homogenous GS expression and increased but non-diffuse sinusoidal CD34 expression in the tumor.

B: Pattern 2: diffuse heterogenous GS expression; GS positive-CD34 negative rim and diffuse sinusoidal CD34 expression in the center of the tumor.

C: Pattern 3: focal patchy GS expression pattern; GS positive-CD34 negative rim and diffuse sinusoidal CD34 expression in the center of the tumor.

D: IHCA without *CTNNB1* mutation showing variable perivascular GS expression in the tumor and unremarkable CD34 expression.

In the non-tumoral liver, there is a normal perivenular GS expression around the central veins and a periportal sinusoidal expression of CD34

R: rim within the HCA, at the margin between tumoral and non-tumoral liver

T: tumor (HCA)

NT: non-tumoral liver

▲ : portal tract

⊙ : central vein

⦿ : Normal GS expression around the central vein

⦿ : normal periportal sinusoidal CD34 expression

Figure 2. Algorithm used in this study, applicable in routine practice

Figure 3. Pattern 1: diffuse homogeneous Glutamine Synthetase (GS) pattern

A, B: Case 66 (b-HCA exon 3 non-S45, large deletion). **A:** strong, homogenous and diffuse expression of GS in the tumor (T), contrasting with the normal expression in non-tumoral liver (NT) limited to a few hepatocytes around central veins (arrow); **B:** sinusoidal expression of CD34 is increased but not diffuse in the T.

Figure 4. Pattern 2: Diffuse heterogeneous Glutamine Synthetase (GS) pattern

A: Case 54 (exon 3 S45 mutated b-HCA) and **B:** case 82 (exon 3 S45 mutated b-IHCA). GS staining is diffuse and heterogeneous in tumor (T), associated with a strong positive GS rim (asterisk) at the border area with non-tumoral liver (NT). Note in B the thick perivascular patches in T (arrow), often observed in case of inflammatory HCA.

C, D: Case 41 (b-HCA ex3 S45). The rim (asterisk) is already vaguely visible at the periphery of T on the H&E (C), and is further confirmed by its CD34 negativity, contrasting with the center of T where CD34 is diffusely expressed in sinusoids (D).

E, F, G: Variations in staining intensity of GS pattern 2: faint GS staining in T (inset), but with a typical rim (E: case 61); moderate intensity (F: case 41); strong intensity (G: case 54).

Figure 5. Pattern 3: Focal patchy Glutamine Synthetase (GS) pattern

A, B: Case 91 (b-HCA ex 7/8). GS staining, almost absent in the tumor (T), underlines a rim at the periphery of the HCA (asterisk) (A); CD34 is diffuse in the tumor sinusoids (T), contrasting with its negativity in the rim (B).

C, D: Case 43 (b-HCA ex 7/8). Very faint GS staining in the center of the tumor (T) associated with a GS positive (C) - CD34 negative (asterisk) rim, contrasting with diffuse CD34 expression in T (D). The faint heterogeneous staining of GS within the tumor may lead to a misinterpretation of pattern 2.

Figure 6. Inflammatory hepatocellular adenoma (IHCA)

A, B: Case 67. The tumor (T) contains some GS patches focally reinforced at the periphery of T (arrow), but without a true rim (**A**); the CD34 sinusoidal staining is unremarkable within T (**B**).

1
2
3
4
5
6
7
8
9
10
11
12
13
14
15
16
17
18
19
20
21
22
23
24
25
26
27
28
29
30
31
32
33
34
35
36
37
38
39
40
41
42
43
44
45
46
47
48
49
50
51
52
53
54
55
56
57
58
59
60
61
62
63
64
65

Table 1. Cases of the series, grouped by molecular categories.

Sample	Age/sex	n / size cm (specific etiology)	IHC diagnosis right/discordance according MA
b-HCA ex3 non-S45		N=6	
42 (T41)*	42/M	1n/10	discordance (S45)
59 (D32-S37)*	14/M	several n/2.7 (androgens)	right
66 (large deletion)*	35/F	1n/12.5	right
68	20/F	1n/5	right
78 (large deletion)*	66/F	1n/6	right
105 (large deletion)*	18/M	adenomatosis/3.8 (glycogenosis type 1)	right
b-HCA ex3 S45		N=13	
11	38/F	1n/6	right
14	29/F	1n/9	right
18	23/F	1n/5.5	right
24*	28/F	1n/16	right
30*	28/F	1n/5	right
41*	24/F	1n/8	right
47*	21/F	1n/9	right
54*	29/F	1n/14	right
61*	21/F	1n/10	right
72	28/F	1n/5.5	right
76	46/F	1n/15	right
92**	28/F	1n/15	right
108	24/F	1n/5.2	right
b-HCA ex 7/8		N=11	
20	34/F	1n/7	right
26*	22/F	1n/13	right
29	29/F	1n/8	right
43*	28/F	1n/2.8	discordance (S45)

56*	28/F	1n/5	discordance (S45)
70	30/F	5n/7	right
77*	24/F	3n/3	discordance (S45)
80	26/F	1n/5	right
88*	27/F	1n/11	discordance (S45)
90 Lausanne	23/F	1n/20	discordance (S45)
91*	24/F	1n/8	right
b-IHCA ex3 non-S45 N=15			
1 (deletion)	23/F	1n/11	right
8 (large deletion)*	32/M	1n/3.5	right
9 (T41)*	35/F	4n/7	right
13 T2 (T41)	33/F	2n/1.8	discordance (S45)
21	27/M	1n/7 (FAPC)	right
22 T4 (A39G)*	46/F	4n/1.5	discordance (S45)
35 T1 (A39G)* <i>same as case 22</i>	46/F	4n/10	right
38 (P52S)	46/F	1n/7	discordance (S45)
39 (D32-S37)*	35/F	1n/3	right
51 (T41)*	26/F	1n/3.5	right
52 (large deletion)*	59/M	1n/13	right
63 T2 (T41)*	44/F	I-adenomatosis/4.2	right
83 (T41)*	38/F	4n/7	right
96 (T41)*	49/M	1n/3.5	right
98 (T41)*	35/M	1n/5.5	right
b-IHCA ex3 S45 N=7			
10	40/F	1n/5	right
28	35/F	1n/4	right
32*	45/F	I-adenomatosis/7	right
82*	29/F	several n/5	right

106*	34/F	1n/8.3	right
107	36/F	1n/8	right
109	21/F	1n/10.5	right
b-IHCA ex7/8 N=11			
3*	46/F	1n/6	right
5*	35/F	1n/10	right
12 T1 <i>same as case 13</i>	33/F	2n/4.4	discordance (IHCA)
17*	53/M	1n/7	discordance (S45)
19*	34/F	1n/8	right
65*	42/F	1n/5	discordance (IHCA)
69*	50/M	1n/10	discordance (S45)
71*	28/M	1n/4	right
74*	51/F	1n/11	right
75*	41/F	1n/4	discordance (S45)
81	19/F	1n/13	right
IHCA N=30			
2	34/F	I-adenomatosis/ 9	right
6	46/F	I-adenomatosis/5.5	right
7	45/F	I-adenomatosis/9	right
23 (T3) <i>same as cases 22, 35</i>	46/F	I-adenomatosis /3	right
27	53/F	1n/15	discordance (b-IHCA 7/8)
33	54/F	1n/8	right
37 (T3)	51/F	I-adenomatosis/3.3	right
40 (T4) <i>same as case 37</i>	51/F	I-adenomatosis/4	right
44	33/M	1n/8	right
48 (T1)	41/F	I-adenomatosis /7	right
49 (T2) <i>same as case 48</i>	41/F	I-adenomatosis /2	right
50	48/F	1n/6	discordance (b-IHCA 7/8)

53	27/F	4n/6	right
57	24/F	1n/8	right
62	31/F	1n/9	discordance (b-IHCA ex3 S45)
64	30/F	1n/10	right
67	36/F	1n/10	right
79	33/F	1n/1.5	right
84 T2 (another nodule was shHCA)	31/F	3n/6	right
87	42/F	1n/3	right
89	50/F	3n/4 (systemic amyloidosis)	right
93	27/F	2/8.7	right
94	50/F	1n/13.5	right
95	47/F	1n/14	discordance (b-IHCA 7/8)
97	21/F	1n/15	right
99	43/F	I-adenomatosis /5	right
101	26/F	1n/13	right
102	26/F	1n/14	right
103	40/F	I-adenomatosis /5	right
104 <i>same as case 27 ; another n 2yrs later</i>	53/F	1n/3.5	right

n : number of HCA present on the surgical specimen

several : number of HCA >4 <10 present on the surgical specimen

adenomatosis : > 10 HCA present on the surgical specimen (including microadenomas <1cm)

I-adenomatosis : inflammatory adenomatosis

size cm : of the HCA reviewed in this study

MA : molecular analysis

* : b-catenin mutation/deletion according to data from ref 11

†: pregnancy cases with severe hemorrhage and HCA rupture

FAPC : familial adenomatous polyposis coli

In italics : different HCA from the same surgical specimen, (except case 104)

Table 2. Summary of the statistical results: molecular analysis (gold standard) versus immunohistochemical analysis of the patterns (consensus).

Molecular analysis	Sensitivity [95%CI]	Specificity [95%CI]	PPV [95%CI]	NPV [95%CI]	AUC [95%CI]
B ex3 non S45	0.83 [0.36-0.99]	1.0 [0.96-1.0]	1.0 [0.48-1.0]	0.99 [0.94-1.0]	0.92 [0.75-1.0]
BI ex3 non S45	0.80 [0.52-0.96]	1.0 [0.95-1.0]	1.0 [0.74-1.0]	0.96 [0.90-0.99]	0.90 [0.80-1.0]
B ex3 S45	1.0 [0.75-1.0]	0.93 [0.84-0.97]	0.68 [0.43-0.87]	1.0 [0.95-1.0]	0.96 0.93-0.99]
BI ex 3 S45	1.0 [0.59-1.0]	0.92 [0.84-0.97]	0.50 [0.23-0.77]	1.0 [0.95-1.0]	0.96 [0.93-0.99]
B ex7/8	0.55 [0.23-0.83]	1.0 [0.96-1.0]	1.0 [0.54-1.0]	0.94 [0.87-0.98]	0.77 [0.62-0.93]
BI ex7/8	0.55 [0.23-0.83]	0.96 [0.90-0.99]	0.67 [0.30-0.93]	0.94 [0.87-0.98]	0.75 [0.60-0.91]
IHCA	0.87 [0.69-0.96]	0.97 [0.89-1.0]	0.93 [0.77-0.99]	0.94 [0.85-0.98]	0.92 [0.85-0.98]

PPV: positive predictive value

NPV: negative predictive value

AUC: area under the curve

B: b-catenin mutation/deletion

I: inflammatory

IHCA: inflammatory hepatocellular adenoma

Figure 1.

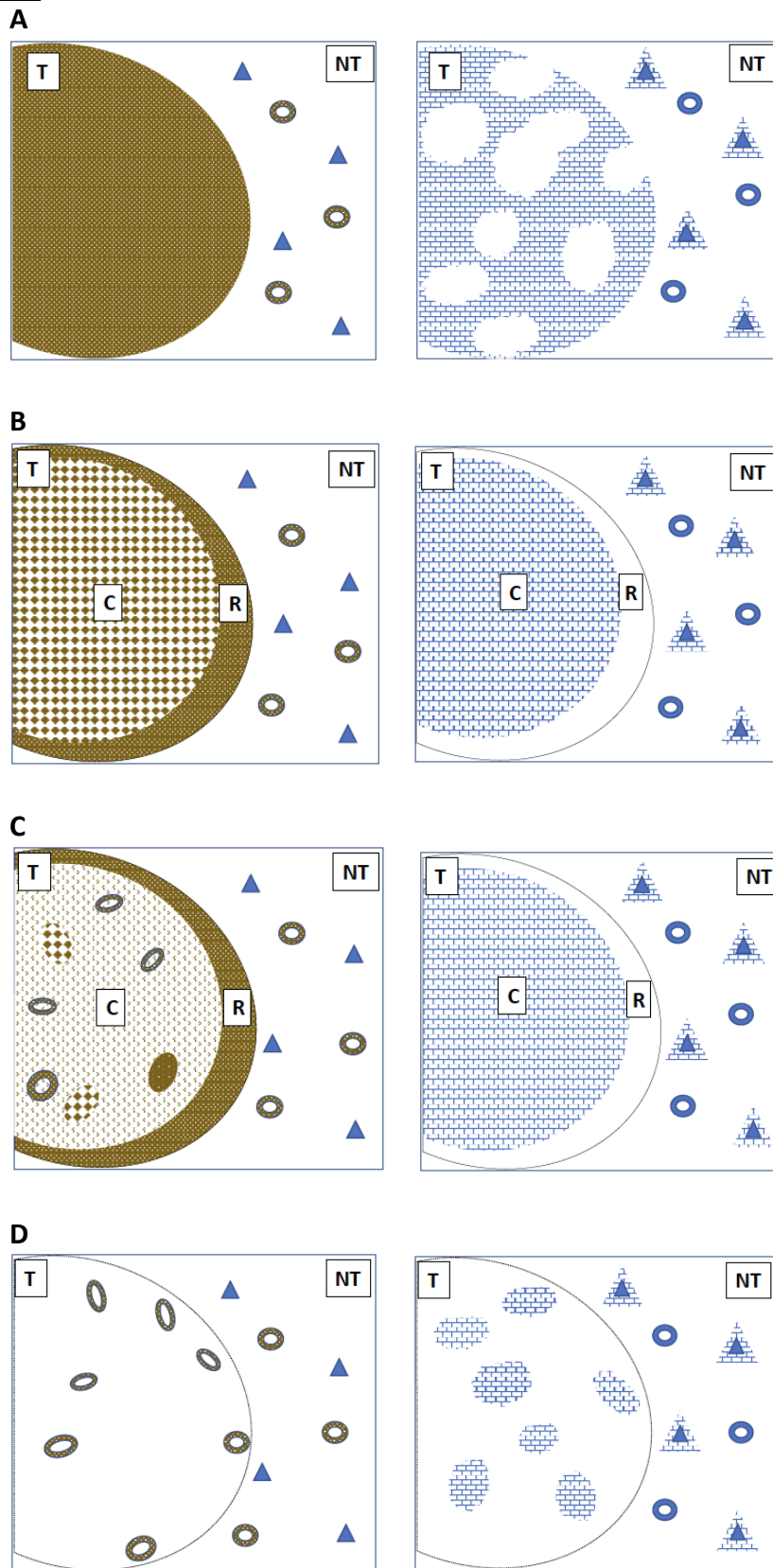


Figure 2

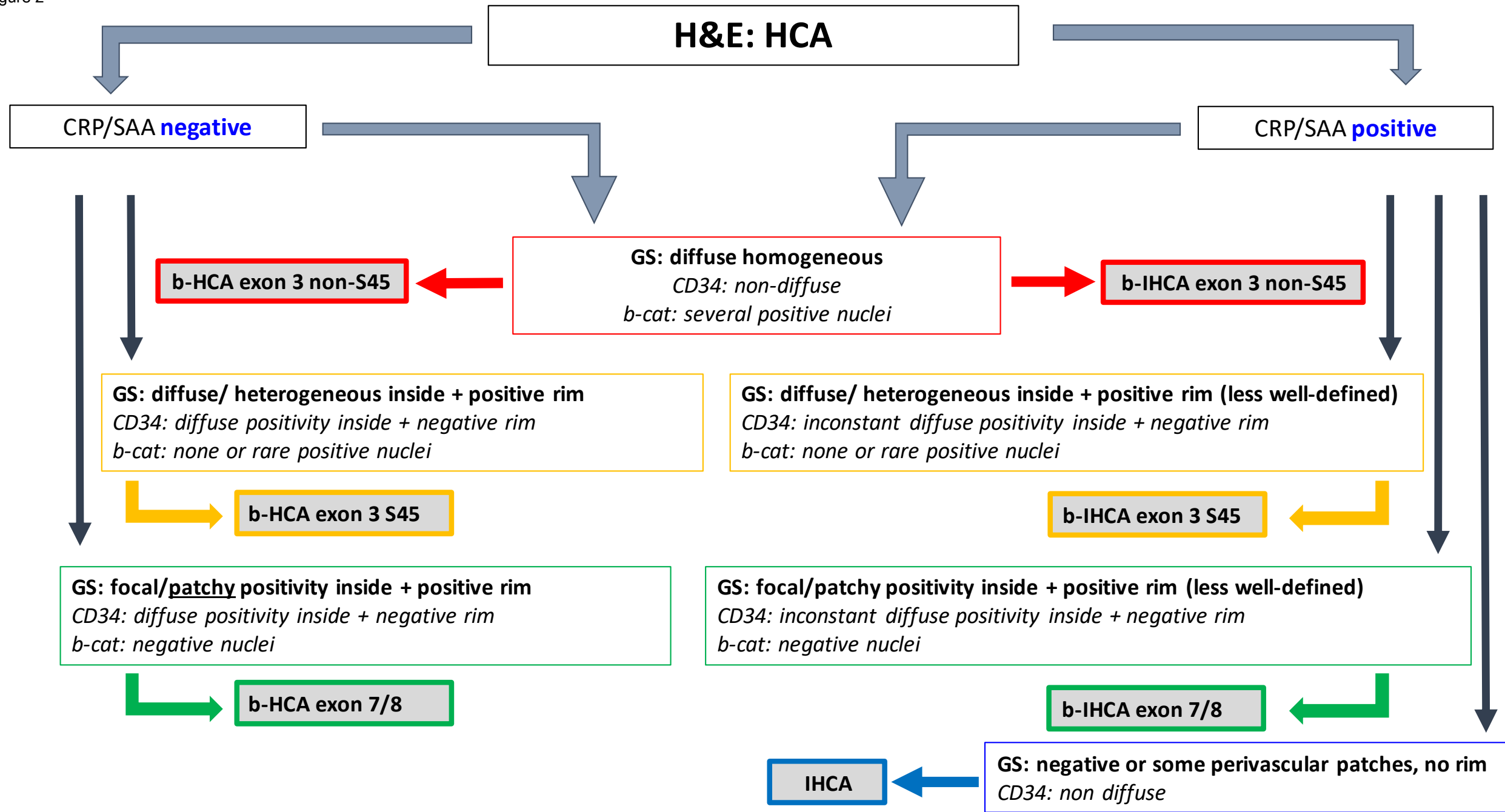


Figure 3

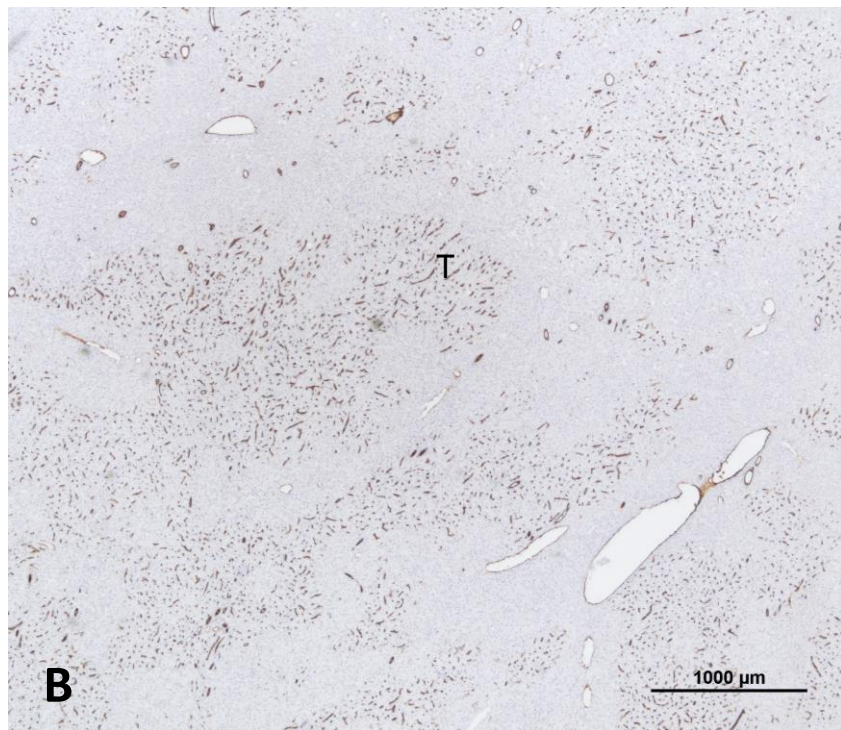
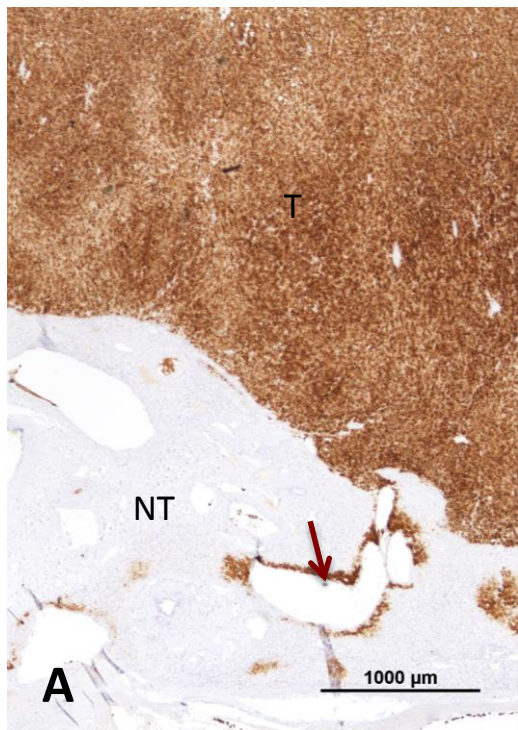


Figure 4

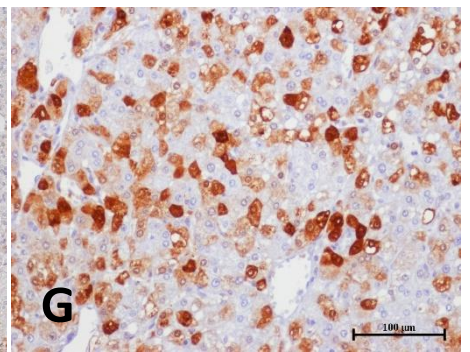
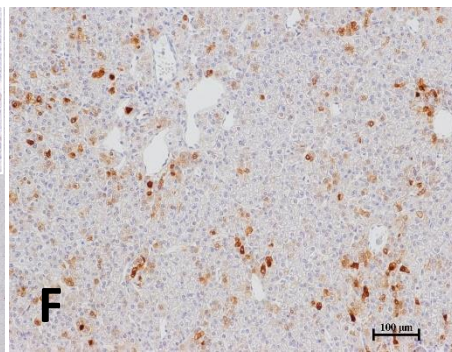
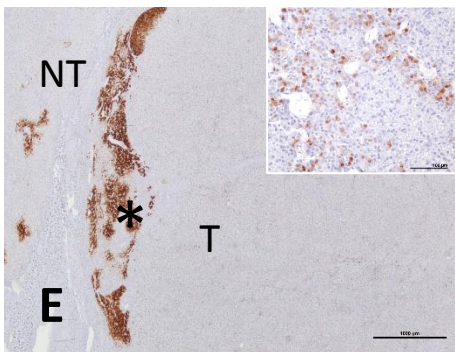
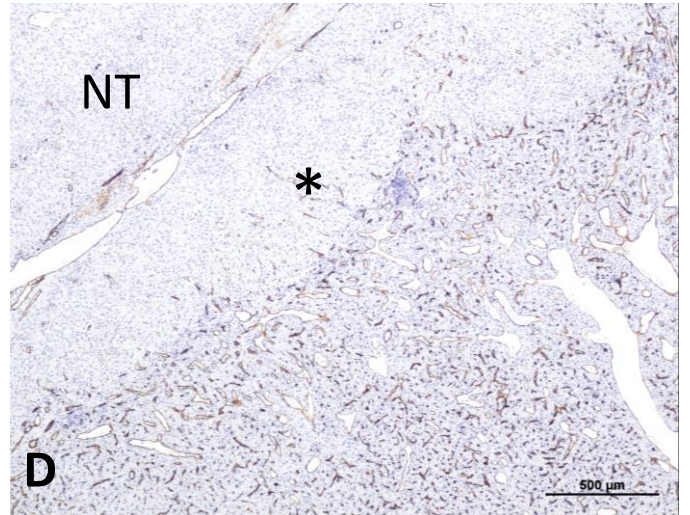
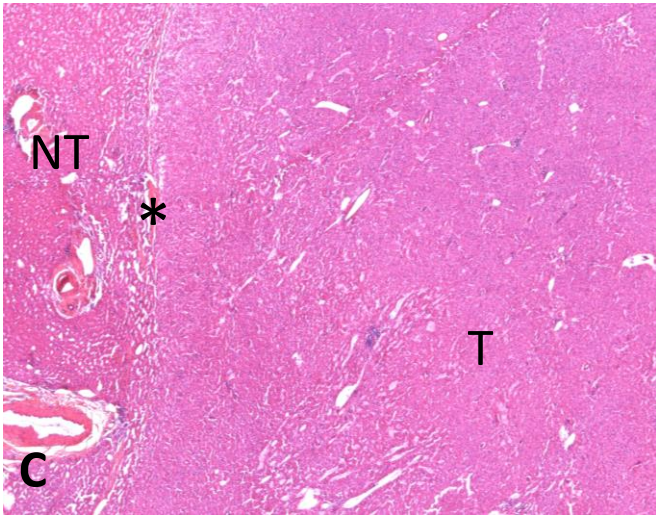
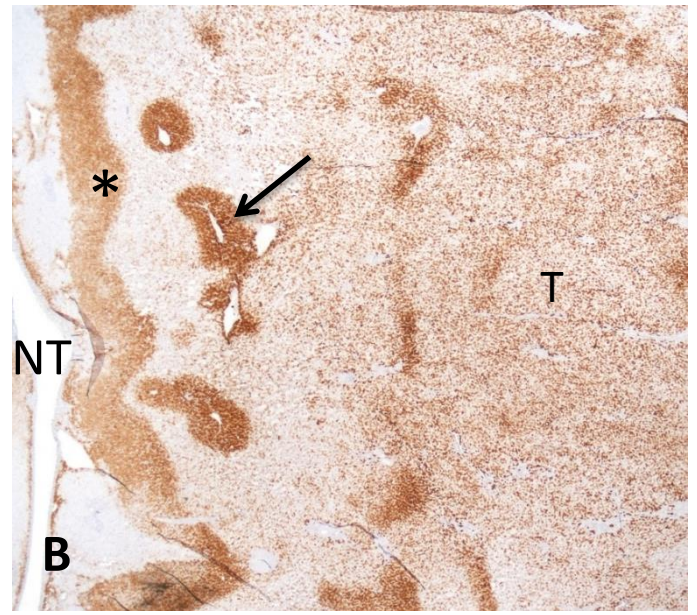
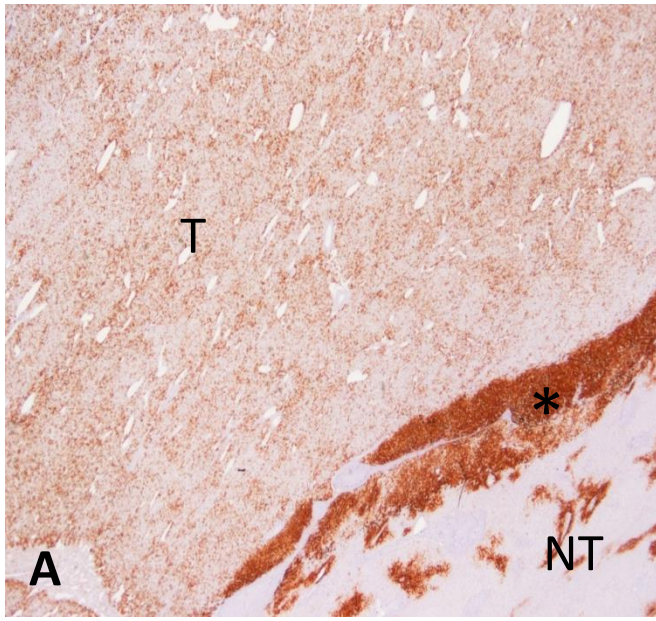


Figure 5

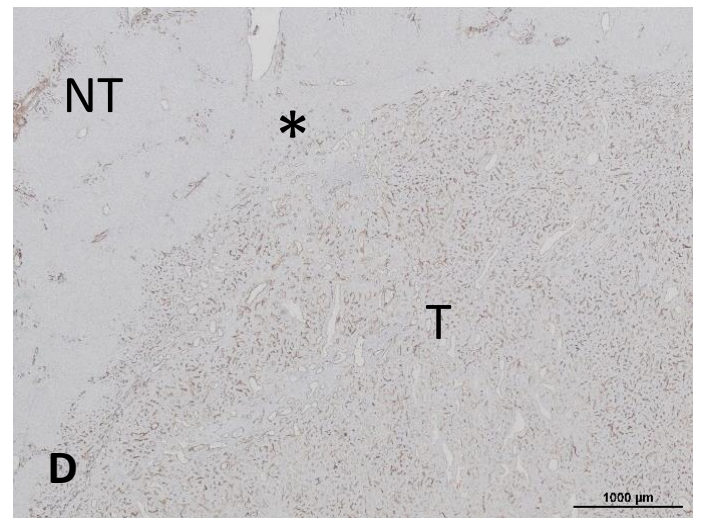
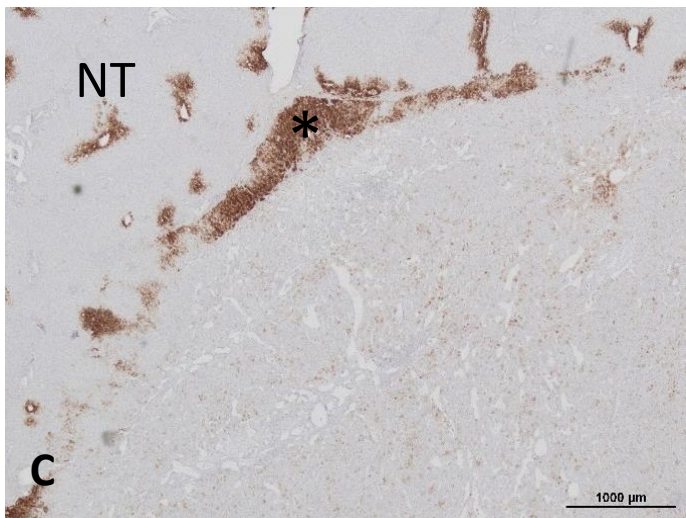
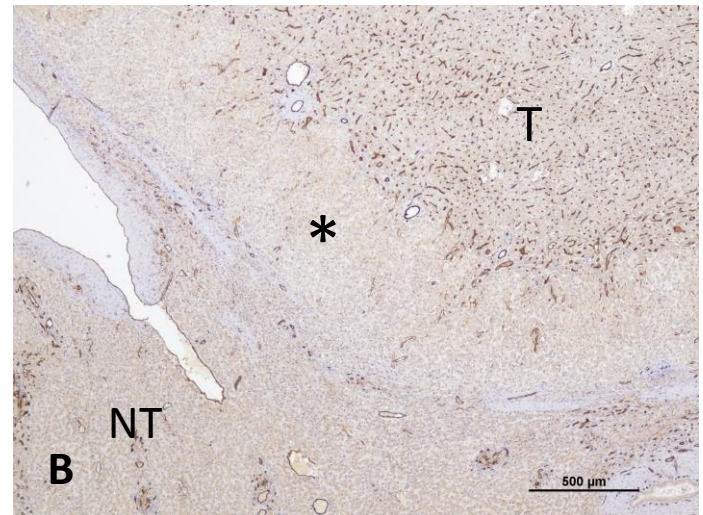
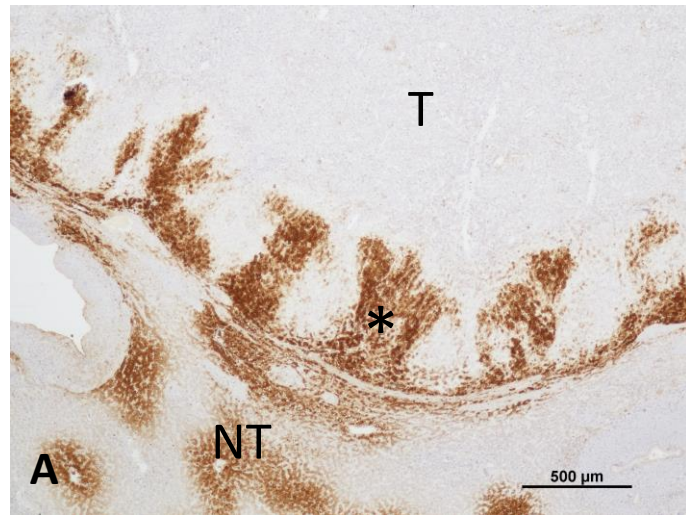


Figure 6

